Thermophysical properties of simple molecular liquid mixtures: On the limitations of some force fields

Abdoul Wahidou Saley Hamani, Jean-Patrick Bazile, Hai Hoang, Han Tuong Luc, Jean-Luc Daridon, Guillaume Galliero

THERMOPHYSICAL PROPERTIES OF SIMPLE MOLECULAR LIQUID MIXTURES: ON THE LIMITATIONS OF SOME FORCE FIELDS.

Abdoul Wahidou Saley Hamani[1], Jean-Patrick Bazile[1], Hai Hoang[2], Han Tuong Luc[2], Jean-Luc Daridon[1], Guillaume Galliero[1*]

[1]Universite de Pau et des Pays de l'Adour, E2S UPPA, CNRS, TOTAL, LFCR, Pau, France.

[2] Institute of Fundamental and Applied Sciences, Duy Tan University, 10C Tran Nhat Duat Street, District 1, Ho Chi Minh City 700000, Viet Nam.

***Corresponding author:** guillaume.galliero@univ-pau.fr

ABSTRACT

In this work, we explore the ability of two force fields, a united atom one (TraPPE-ua: Transferable Potential for Phase Equilibria united atom) and a coarse grained one (MCCG: Mie chain Coarse Grained), to describe simultaneously equilibrium derivative properties, such as isothermal compressibility and speed of sound, excess property in mixtures and transport properties such as shear viscosity in binary liquid mixtures composed of n-hexane + n-dodecane over a wide range of thermodynamics conditions (from 293.15 to 353.15 K and pressure up to 100 MPa). To do so on a consistent and controlled set of experimental data, we have measured accurately density, speed of sound and shear viscosity of these mixtures. Numerically, we computed the aforementioned thermophysical properties at the same thermodynamic conditions using both classical Monte Carlo and Molecular Dynamics simulations. Comparisons between experimental data and molecular simulations of volumetric and acoustic properties indicate a fair agreement for both force fields, with an overall advantage to the MCCG force field. In addition, both approaches, combined with classical Lorentz-Berthelot combining rules, are able

to capture reasonably well the small excess properties of the studied thermodynamic properties. However, non-negligible deviations, up to around 50 %, are observed on viscosity for the densest systems. Such deviations confirm that, even on simple molecular systems, force fields may be limited to yield precise transport properties at high densities.

Keywords: Thermophysical properties, Shear viscosity, High pressures, normal alkane, Monte Carlo, Molecular Dynamics.

1. INTRODUCTION

Mixtures of molecular fluids, such as hydrocarbons ones, are widely present in the industry. Therefore, the thermophysical characterization of these mixtures is of primary importance to optimize the related processes. Despite the great interest for this question, it remains a topical issue considering that the predictive approaches (equations of states, mixing rules, correlations) are not always able to provide satisfactory results in particular when dealing with derivative thermophysical properties[1–3] or transport properties such as viscosity[4,5] under high pressures as found in the oil and gas industry.

Molecular simulation is a complementary tool[6] to deal with the thermophysical properties of such molecular systems over a wide range of thermodynamic conditions. Previous works[1,6–12] showed that it is possible to predict with a good accuracy the thermodynamic properties of hydrocarbon molecules and their mixtures, even when using these simulation techniques combined with force fields based on a coarse grained representation. However, it seems less clear whether such approaches are able to provide simultaneously derivative properties like speed of sound, excess properties in mixtures, and transport properties like viscosity even for simple molecular fluids such as hydrocarbons[10,13,14].

Thus, in this work, which deals with liquid binary mixtures of n-hexane and n-dodecane, we have evaluated the ability of two force fields to provide equilibrium properties (density, isothermal compressibility, speed of sound), the corresponding excess properties, and transport (viscosity) properties over a wide range of thermodynamic conditions (from 293.15 to 353.15K and pressure up to 100 MPa). To do so we have chosen a widely used united atom force field, the Transferable Potential for Phase Equilibria (TraPPE-ua)[8] and a recently developed coarse grained force field, the Mie Chain Coarse Grained (MCCG)[9,11] for which an accurate equation of state has been developed[12]. To perform the comparison on a consistent and controlled set of

experimental data, we have measured accurately density, speed of sound and shear viscosity of these mixtures.

The first section of the article is devoted to a brief description of the experimental setups used for measurements. Additional details are provided in the Supplementary Information (SI) file. Then, are detailed the two different force fields used in the molecular simulations, the simulation protocol and some numerical details. In the results part, for each studied property, we systematically compare and discuss the experimental data and the simulations results. Finally, we summarize the main outcomes of this study in the last section.

2. MATERIAL AND METHODS

2.1. Experimental details

2.1.1. Chemicals

Normal-hexane (purity > 99%, with a certificate of analysis of 99.98%) and normal-dodecane (purity > 99%, with a certificate of analysis of 99.98%) were obtained from Sigma Aldrich. Both components were used without any further treatment.

2.1.2. Density Measurement and Isothermal Compressibility Calculation

Density measurements were carried out by using a U-tube density meter. To control and measure the pressure of the system, we have used a piston pump and a Presens manometer with a standard uncertainty of $\pm 0.02\%$, respectively. The thermal regulation of the system was attained by using a thermostatic bath, and the temperature was measured with a Pt100 thermometer with a standard uncertainty of 0.03 K. Calibration was achieved by the protocol proposed by Lagourette et al.[15] using vacuum and deionized water. The standard uncertainty of each measured density value was estimated according to the GUM of NIST[16] by combining the quadratic sums of the different sources of uncertainty present in the working equation. Uncertainty evaluation was presented in detail in this paper[17]. Isothermal compressibility κ_T

was determined by deriving experimental density data, using a computational procedure developed by Daridon and Bazile[17]. This procedure is based on a Monte Carlo method which uses 5000 trials to obtain the property and the associated combined standard uncertainty. The calculated compressibility exhibits relative deviations that reach, at most 1 %.

2.1.3. Speed of Sound Measurement:

The speed of sound measurements were performed by a pulse-echo technique working at a resonant frequency of 3 MH_z in the reflection mode as described in a previous paper[18]. The pressure of the system was measured by a pressure transducer with an uncertainty of 0.01 MPa, mounted between the pump and the high pressure vessel. The thermal regulation is insured by immerging the high pressure cell within a thermostatic bath of stability 0.02 K. The temperature measurement was made using a Pt 100 probe with an uncertainty less than 0.1 K, placed inside the cell. As for density, the standard uncertainty of the speed of sound value is estimated according to the GUM of NIST, see SI for details.

2.1.4. Viscosity Measurement

Viscosity were measured under pressure using a vertical falling body viscometer as described in ref.[19]. The pressure is measured using a metal gauge sensor connected to a digital display whose accuracy is of $\pm$ 0.01 MPa at atmospheric pressure and $\pm$ 0.1MPa for pressure up to 100 MPa. The thermal regulation of the system is carried out using a thermostatic bath Huber Unistat CC. The temperature acquisition was made using a platinum probe 100 Ω, placed inside the measurement cell and connected to a display AOIP PN5207 with an uncertainty of $\pm$ 0.1K. The expanded uncertainty in viscosity obtained by this method is are estimated according to the GUM of NIST.

2.2. Molecular simulation details

2.2.1. Force Fields

In this section, we present the two force fields considered in this work: a united atom force field[20] called Transferable Potential for Phase Equilibria united atom (TraPPE-ua) proposed by Martin and Siepmann[8] and a coarse grained model[20,21] named Mie Chain Coarse Grained (MCCG) developed by Hoang et al.[9]. It should be noticed that, beyond the difference in their functional forms and the details of the corresponding molecular description, the two force fields also present a difference in their parameterization protocol. More precisely, the parameters of TraPPE-ua are determined by, to the first order, a minimization of the errors on the critical temperature and on some data of saturated liquid densities[8], whereas for MCCG, parameters are directly and univocally computed from the critical temperature, one saturated liquid density, the acentric factor and one saturated liquid viscosity, using a corresponding states approach[9], similarly to what proposed by Mejia et al[11].

Thus, MCCG parameterization is straightforwardly achieved without fitting and requires less data than what is required to fit TraPPE-ua parameters, but requires one data on shear viscosity contrary to TraPPE-ua parameterization. It should be noticed that the MCCG parameterization could be achieved as done for the TraPPE-ua, i.e. by minimizing the error with a set of data, but a corresponding states strategy could not be used to adjust the TraPPE-ua parameters as they are too numerous. Both strategies possess strengths and weaknesses but, including a transport property, in addition to equilibrium ones, in the parameterization strategy allows to better constrain the molecular model as already shown [9,13,22-23] when dealing both with equilibrium and transport properties.

Furthermore, it is worth noticing that the choice of the MCCG was motivated not only because it is interesting to look at the capabilities/limitations of a coarse grained force field but also because an equation of state already exists to describe rather accurately its equilibrium

properties[12]. This could replace molecular simulations in some circumstances, even if this is out of the scope of this work.

TraPPE-ua

The description of n-hexane and n-dodecane molecules with the TraPPE-ua model relies on two united-atom groups: CH_3 and CH_2, i.e. the hydrogen atoms are not explicitly described. The non-bonded interactions are described by a pairwise additive Lennard-Jones (LJ) 12-6 potential[24,25]:

$$U_{NB}(r_{ij}) = 4\varepsilon_{ij}[(\frac{\sigma_{ij}}{r_{ij}})^{12} - (\frac{\sigma_{ij}}{r_{ij}})^{6}] \quad (1)$$

where, r_{ij} is the distance between i^{th} and j^{th} particles, ε_{ij} and σ_{ij} are the LJ interaction parameters representing the depth of LJ potential well and the size of particles, respectively. The LJ interaction parameters are given in Table I.

For unlike non-bonded united-atoms, the LJ parameters are determined using the standard Lorentz-Berthelot combining rules[26,27]:

$$\sigma_{ij} = \frac{(\sigma_{ii}+\sigma_{jj})}{2} \quad (2)$$

$$\varepsilon_{ij} = \sqrt{\varepsilon_{ii}\varepsilon_{jj}} \quad (3)$$

Table I. Parameters used for the TraPPE-ua force field. The subscript *x* and *y* are equal to 2 or 3

United-atom	σ_{ij}[Å]	ε_{ij}/K_B [K]
CH_3 (SP3)	3.75	98
CH_2 (SP2)	3.95	46
Stretch[a]	r_{eq}[Å]	K_r/k_B[K.Å^{-2}]
CH_x-CH_y	1.54	452900

Bending	θ_{eq}[deg]	K_θ/k_B[K.rad^{-2}]		
CH_x-CH_2(sp3)-CH_y	114	62500		
Torsion	c_0/k_B [K]	c_1/k_B [K]	c_2/k_B [K]	c_3/k_B [K]
CH_x-CH_2-CH_2-CH_y	0.00	355.03	-68.19	791.32

[a] Stretch parameters taken from Mundy et al.[26].

Adjacent particles are connected by a bond. Originally, the TraPPE-ua force field considers the bond to be fixed at 1.54 Å for n-alkanes. This type of bond is very convenient in implementing Monte Carlo simulations but not Molecular Dynamic simulations[29]. To tackle this problem, a harmonic bond-stretching potential was used to describe the bond for MD simulations as recommended by Kelkar et al.[29]:

$$U_{stretch} = \frac{K_r}{2}(r - r_{eq})^2 \quad (4)$$

where, r is the distance between adjacent particles, r_{eq} and K_r are parameters of the harmonic bond stretching potential to represent equilibrium bond length and the force constant, respectively. Hence, in this work, we have used the fixed bond in the MC simulations and the harmonic bond in MD simulations. Since TraPPE-ua force field was not provided with bond stretching constants, we used the ones from Mundy et al.[28], listed in Table I. This modification of the force field is known to have a negligible effect on the performance of the force field[29].

Two adjacent bonds form a bond angle θ whose motion is governed by a harmonic potential:

$$U_{bend} = \frac{K_\theta}{2}(\theta - \theta_{eq})^2 \quad (5)$$

Where θ_{eq} and K_θ, listed in Table I, are the equilibrium bending angle and the force constant, respectively.

The torsional potential interactions for particles separated by three bonds is described by a cosines series as follows:

$$U_{torsion} = c_0 + c_1(1 + \cos(\emptyset)) + c_2(1 - \cos(2\emptyset)) + c_3(1 + \cos(3\emptyset)) \quad (6)$$

Where $\emptyset$ is the dihedral angle and $c_{i=0:3}$ are the Fourier coefficients. Values of these coefficients are given in Table I.

Mie Chain Coarse Grained

The molecular representation with the Mie Chain Coarse Grained force-field consists in using homo-nuclear chains composed of N freely jointed spheres. Interaction between two non-bonded spheres i and j is described by the Mie λ-6 potential[30,31]:

$$u_{Mie}(r_{ij}) = \left(\frac{\lambda_{ij}}{\lambda_{ij}-6}\right)\left(\frac{\lambda_{ij}}{6}\right)^{6/(\lambda_{ij}-6)} \varepsilon_{ij}\left[\left(\frac{\sigma_{ij}}{r_{ij}}\right)^{\lambda_{ij}} - \left(\frac{\sigma_{ij}}{r_{ij}}\right)^{6}\right] \quad (7)$$

where λ_{ij} is the exponent characterizing the repulsive interactions between non-bonded spheres. The parameters of MCCG force field for n-hexane and n-dodecane are listed in Table II.

Table II . Mie Chain Coarse Grained (MCCG) parameters of n-hexane and n-dodecane.

Molecules	N	σ_{ii} (Å)	ε_{ii}/k_B [K]	λ_{ii}
n-hexane	3	3.862	267.88	13.38
n-dodecane	5	4.025	336.33	15.84

In the case of mixtures, the cross-interaction parameters σ_{ij}, ε_{ij} and λ_{ij} were determined by using the same combining rules as in the work on the development of the MCCG for field [9] and related works[32-34]. They are simple and seems able to yield good results for various thermophysical properties of weakly asymmetric mixtures[9,31], even for subtle properties depending strongly on cross interactions, such as thermal diffusion factors[31,34]. More precisely, σ_{ij} and ε_{ij} are calculated using the classical Lorentz-Berthelot combining rules as previously defined in Eqs. (2) and (3), and the repulsion exponent of the cross-interactions, λ_{ij}, is evaluated using an arithmetic average as:

$$\lambda_{ij} = \frac{\lambda_{ii}+\lambda_{jj}}{2} \quad (8)$$

It should be noticed that there exist other possibilities regarding the combining rule on the repulsion exponent[12,32], and that a careful analysis of its impact on the results would deserve a dedicated work. However, for the studied system, the asymmetry on the repulsion exponent is relatively limited, see Table II, and a different choice of the combining rule leads to cross repulsion exponents which are very similar.

2.2.2. Methodology and simulation details

Thermodynamic properties

To estimate the thermodynamic properties, we have performed Monte-Carlo (MC) molecular simulations in the isothermal-isobaric ensemble (NPT). The simulation boxes were cubic and contain at least 200 molecules for the TraPPE-ua force field and at least 400 molecules for the MCCG force field. The classical periodic boundary[20,21] conditions were applied in all directions. The non-bonded interactions were truncated at a cut-off radius of 14A° for the TraPPE-ua force field[8] and $4.5\sigma_{ij}$ for the MCCG force field[9], and the long range corrections (LRC) were included. In the simulations, four MC moves[20,21,35] were implemented: (1) volume change, (2) molecular translation, (3) molecular rotation and (4) configurational-bias MC partial regrowth[36–38].

All MC simulations consisted of two steps. First, the systems were equilibrated during a run of more than 5×10^6 MC moves. During the equilibration step, maximum amplitudes of the first three MC moves were adjusted so that the acceptance rates of these moves were approximately of 50%. Then, the samplings were performed during at least 3×10^7 MC moves to compute the thermodynamic properties.

Density was directly calculated by averaging its instantaneous values over MC moves as:

$$\rho = \left\langle \frac{\sum_i N_i \times M_i}{V} \right\rangle \quad (9)$$

where, N_i and M_i are numbers of molecules and molecular mass of i^{th} compound, respectively, V is the volume, and $\langle ... \rangle$ denotes an average over MC moves.

For the isothermal compressibility, we used the fluctuation theory[20,39] to estimate it during the simulations, using:

$$\kappa_T = -\frac{1}{\langle V \rangle}\left(\frac{\partial \langle V \rangle}{\partial P}\right)_T = \frac{1}{\langle V \rangle k_B T}(\langle V^2 \rangle - \langle V \rangle^2) \quad (10)$$

where, k_B is the Boltzman constant.

The speed of sound was deduced from other thermodynamic properties via Newton-Laplace equation[40] as:

$$w = \frac{1}{\sqrt{\rho(\kappa_T - \frac{TM\alpha_P^2}{\rho c_p})}} \quad (11)$$

where, α_p is the isobaric thermal expansion and c_p is the molar isobaric heat capacity. The fluctuation theory has been used to compute α_p during the simulations[1] as:

$$\alpha_P = \frac{1}{\langle V \rangle}\left(\frac{\partial \langle V \rangle}{\partial P}\right)_T = \frac{1}{\langle V \rangle k_B T^2}\left(\langle V\widehat{H} \rangle - \langle V \rangle \langle \widehat{H} \rangle\right) \quad (12)$$

where, $\widehat{H}$ is the configurational enthalpy: $\widehat{H} = U^{ext} + U^{int} + PV$, where U^{ext} and U^{int} are the intermolecular and intramolecular potential energy, respectively.

Regarding the molar isobaric heat capacity, it is decomposed in an ideal and residual isobaric heat capacities in which the former is determined from the NIST database[41] and the latter is quantified during the simulations thanks to the fluctuation theory[1] as:

$$c_P^{res} = \left(\frac{N_a}{k_B N T^2}\left(\langle U^{ext}\widehat{H} \rangle - \langle U^{ext} \rangle \langle \widehat{H} \rangle\right) + \frac{N_a P}{k_B N T^2}\left(\langle V\widehat{H} \rangle - \langle V \rangle \langle \widehat{H} \rangle\right) - N_a k_B \right) \quad (13)$$

where, N_a is the Avogadro number.

The MC molecular simulations have been carried out by modifying the Towhee-7.1.0 MCCCS (Monte Carlo for Complex Chemical System)[42] package for the TraPPE-ua force field and using an in-house code[9] for the MCCG force field. The standard deviations have been estimated using the sub-block average method[21] for the properties computed directly (ρ, κ_T, α_P and c_p^{res}).

Concerning the derived properties such as the speed of sound and excess properties (as defined later), their uncertainties were simply computed by propagating standard deviations of properties directly provided from the simulations. It is worth noting that the uncertainties of the derived properties obtained by this way may be large, even of the same magnitude as their values for the excess properties of weakly asymmetric mixtures. To improve these uncertainties, a straightforward method is to perform independent simulations in each of which the derived properties are calculated. Then, their uncertainties are estimated from values of independent simulations. However, this requires numerous simulations and so has not been employed in this work

Viscosity computation

The shear viscosity was computed by performing Molecular Dynamics (MD) simulations. To do so, we employed the reverse non-equilibrium molecular dynamics (RNEMD) method proposed by F. Müller-Plathe[43]. In this method, the simulation box was divided into n_{slab} slabs along the z direction, then a bi-periodic linear momentum flux was imposed by exchanging momentum along the x direction of atoms every N_{swap} time steps. More precisely, at the exchange time step, an atom in the 1st slab with the most negative x velocity component (v_x) exchanged this component with the one of an atom in the $(n_{slabs}/2)^{th}$ slab that has the most positive x velocity component. To keep the periodic boundary condition in the z direction, a similar exchange was also applied between $(n_{slabs})^{th}$ slab and $(n_{slabs}/2 + 1)^{th}$ slab. This momentum transfer implied a velocity gradient in the simulation box. The linear momentum flux, i.e. the shear stress, induced by this exchange was determined as:

$$j_z(p_x) = \frac{\Delta P_x}{2tL_xL_y} \quad (14)$$

where, ΔP_x is the total exchanged momentum during the time t, L_x and L_y are the lengths of the simulation box in the x and y directions, respectively.

When the system reached the steady state, the shear viscosity was estimated by using the Newton's law of viscosity as:

$$\eta = -\frac{j_z}{(\partial v_x/\partial z)} \tag{15}$$

where, $\partial v_x/\partial z$ is the shear rate which was computed from the velocity profile. It is worth noting that if the momentum flux j_z is large, which corresponds to small values of N_{swap} , the velocity profile could be non-linear, so the system is in a non-linear response regime (shear thinning regime for instance). Hence, to ensure that the particle swapping frequency (N_{swap}) used for each run was sufficiently small to be in a linear-response regime, we checked its effect on the shear viscosity, see details in section II.1 of the SI file.

All MD simulations consisted of three steps. In a first step, the systems were equilibrated during a run of more than 1×10^6 time steps. Then, in a second step, the RNEMD method was applied to shear the fluid during at least 1×10^6 time steps. In a last step, the system reached the steady state, a run of more than 6×10^6 time steps was used to perform samplings.

Simulation boxes contained at least 300 molecules for the TraPPE-ua force field and at least 600 molecules for the MCCG force field, and were designed such that $L_z = 2L_x = 2L_y$. Classical periodic boundary conditions were applied in all directions. The cut-off radii were used to be equal 14A° and $4.5\sigma_{ij}$ respectively for the TraPPE-ua and MCCG force field, and the long range corrections were included. The velocity Verlet algorithm was employed to integrate the equations of motion. To keep the temperature constant, thermostat algorithms (Nose-Hoover[44–46] for TraPPE-ua force field and Berendsen[47] for MCCG force field) were applied to all three velocity components (*x*, *y*, and *z*) during the equilibrium MD simulations, whereas they were applied only to y and z velocity components during the NEMD simulations, in order not to introduce a bias in the flow direction, *z*. To constrain the bond length in the MCCG force field, we employed the classical RATTLE algorithm[48]. Molecular Dynamic simulations are implemented using the LAMMPS package[49] for the TraPPE-ua force field and

an in-house code[9] for the MCCG force field. Standard deviations were estimated using the sub-block average method[21].

3. RESULTS AND DISCUSSION

To achieve a consistent and controlled comparison of molecular simulations results with experimental data we have performed some dedicated experiments. Experimental measurements of density, speed of sound and viscosity were performed on pure n-hexane and n-dodecane and on four binary mixtures of these components at mole fractions of 20, 40, 60 and 80 % of n-hexane. Measurements were carried out along four isotherms spaced at 20 K intervals in the temperature range of 293.15-353.15 K at pressures ranging from 0.1 to 100 MPa by steps of 10 MPa, except for the isotherm at 353.15 K where the minimum pressure is 10 MPa for the n-hexane and the four binary mixtures. For this isotherm, atmospheric measurements were not carried out in order to avoid possible evaporation of the n-hexane. All experimental data used for comparison with molecular simulations are provided in the SI file. The quality of the measurements was validated by comparing data obtained for pure component to reference correlations available in the literature for both components. The comparison plots, provided along with experimental data in the SI file (see Figs. S.1 to S.6.), indicate that our experimental measurements data are consistent with those provided in the literature.

3.1.Thermodynamic properties

3.1.1. Density

Monte Carlo simulations of densities were performed at the same conditions (*P, T, x*) than the experimental measurements so as to allow comparisons. The simulation results and the corresponding standard errors are listed in Tables S.7 and S.8 of SI for TraPPE-ua and MCCG, respectively. For both force fields, a reasonable agreement is observed between the computed and experimental density data but with a systematic overestimation as shown in Fig. 1. The

observed deviations become larger as the system is denser whatever the force field. Consequently, reducing n-hexane content deteriorates the simulations results. Similarly, decreasing temperature or increasing the pressure negatively affects the accuracy of the simulation results as depicted in the different panels of Fig. 2. Quantitatively, the MCCG force field provides results that are slightly better than those of the TraPPE-ua. More precisely, for TraPPE-ua, the overall Absolute Average Deviation (AAD) over the full pressure and temperature range is 1.5%, the overall relative deviation (Bias) is -1.5 % and the Maximum Absolute Average Deviation (Max AD) is 3.0 %. Whereas for MCCG, we observed an AAD of 1.2 %, a Max AD of 2.2 % and a Bias of -0.5 %.

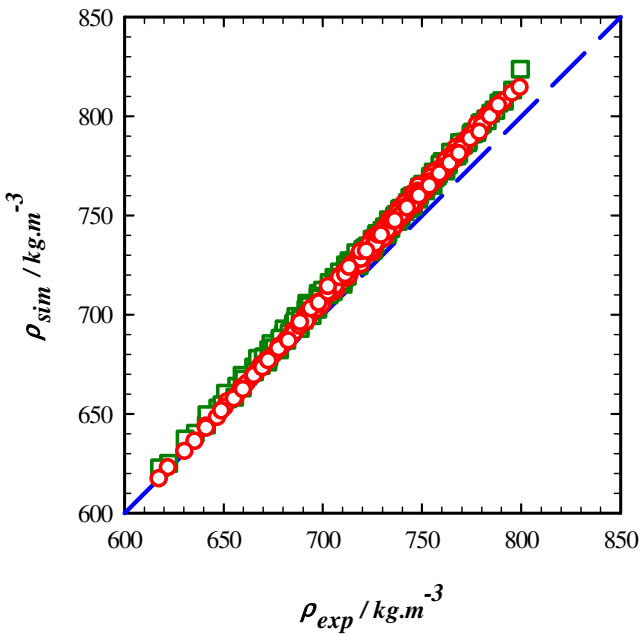

Fig. 1. Molecular simulation data of density ρ_{sim} as a function of experimental density data ρ_{exp} for the mixture n-hexane + n-dodecane. Comparison between □: TraPPE-ua and ○: MCCG. Dashed line represents the reference, i.e. $\rho_{sim} = \rho_{exp}$.

To highlight the mixing behavior of the system, the excess molar volume of the binary mixture was calculated from densities by using the following equation:

$$v^E = \frac{x_{nC6}M_{nC6}+(1-x_{nC6})M_{nC12}}{\rho} - \left(\frac{x_{nC6}M_{nC6}}{\rho_{nC6}} + \frac{(1-x_{nC6})M_{nC12}}{\rho_{nC12}}\right) \quad (16)$$

Where x_{nC6} is the mole fraction of n-hexane, M_{nC6} and M_{nC12} the molecular weights of n-hexane and n-dodecane respectively, and ρ, $\rho_{nC6}$and ρ_{nC12} the density values of the binary mixture, n-hexane and n-dodecane, respectively.

As expected for such a type of paraffin mixtures, the excess molar volume values are small (i.e. below 1% of the total molar volume) and are globally negative. This trend is related to the lodgment of n-hexane molecule[50] in the interstices formed by the larger n-dodecane molecules, thus decreasing the free volume of the real mixture, an effect which is here slightly larger than the positive one due to weak dipole-induced dipole-induced interactions between the two constituents. Moreover, it has been found that v^E increases by increasing the temperature at fixed pressure and decreases by increasing the pressure at a given temperature. Excess molar volumes are also calculated from simulations results of density by applying Eq. (16). In general, both of the force fields provide results in quantitative agreement with those obtained from experiment. Fig. 3 compares the experimental relative excess molar volumes (v^E/v) to that obtained from simulation densities for conditions where the most pronounced effect are observed, i.e. T = 313.15 K and P = 0.1MPa. It is shown in this figure that simulation values are consistent with experimental data despite a systematic underestimation of the absolute values. Thus, the weak non-ideality of the studied binary mixture, from the excess molar volume point of view, is reasonably well captured by the simulations, meaning that the simple Lorentz-Berthelot rule combined with the tested force fields seems sufficient for such mixtures and properties, even if not perfect. This result confirms that the misevaluation of the density by molecular simulations, shown in Figs. 1 and 2, is not due to the combining rules but to the limitations of the tested force fields to model very finely the pure components densities, in particular the n-dodecane one.

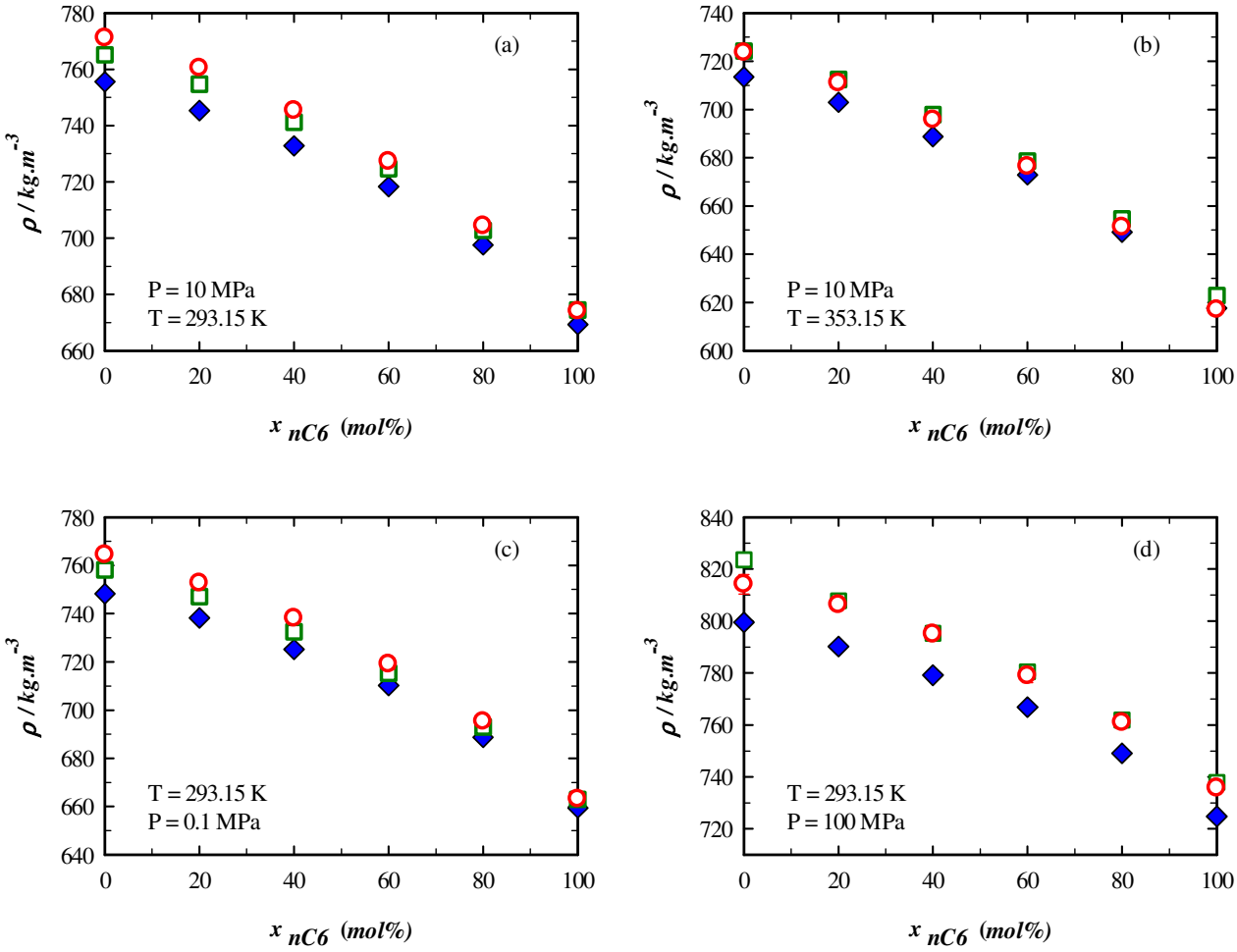

Fig. 2. Density as a function of n-hexane concentration at different temperature and pressure conditions. Comparison between ◆ : experimental data; □: TraPPE-ua and ○: MCCG. The simulation error bars are too small to appear on the graphs.

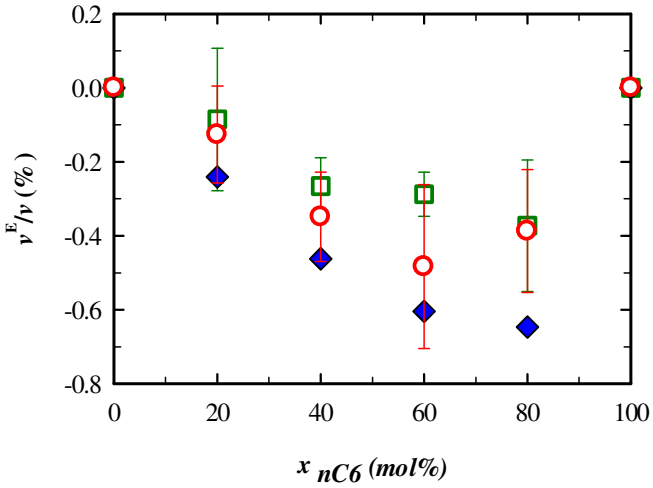

Fig. 3 Relative excess molar volume as a function of concentration of n-hexane at 333.15 K and 0.1 MPa. Comparison between data calculated from ◆: experimental data; □: TraPPE-ua and ○: MCCG .

3.1.2. Isothermal compressibility

Simulations results of isothermal compressibility obtained from fluctuation theory[20,39] are reported in **Tables S.9 and S.10** of SI file**.** Comparisons of these results to experimental ones presented in Figs. 4 and 5 indicate that both of the force fields compute reasonably well this derivative quantity. From a qualitative point of view, we can notice in Figs. 4 and 5 a systematic overestimation of κ_T by the TraPPE-ua force field while for MCCG the simulation results randomly fluctuate around the experimental data. More precisely, we have obtained an AAD of 11.1 %, a Bias of -11.1 % and a Max AD of 28.3 % for TraPPE-ua and an AAD of 5.9 %, a Bias of -3.2 % and a Max AD of 22.7 % for MCCG. This indicates, as found on densities, that the MCCG performs better than the TraPPE-ua to describe isothermal compressibilities.

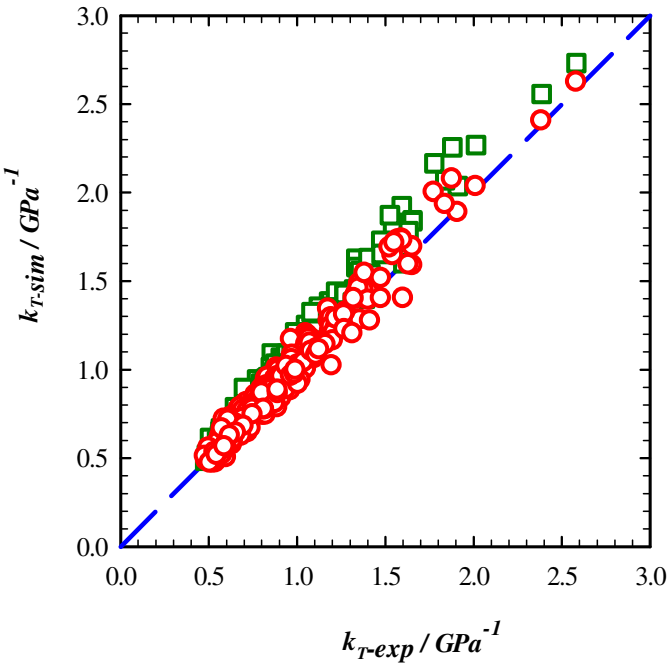

Fig. 4 Molecular simulation data of isothermal compressibility κ_{T-sim} as a function of experimental data κ_{T-exp} for the mixture n-hexane + n-dodecane. Comparison between □: TraPPE-ua and ○: MCCG. Dashed line represents the reference, i.e. $\kappa_{T-sim} = \kappa_{T-exp}$.

To highlight the mixing effect of the studied mixture in terms of κ_T, we calculated the excess isothermal compressibility from the following relation[51]:

$$\kappa_T^E = \kappa_T - \emptyset_{nC6}\kappa_{T,nC6} - (1 - \emptyset_{nC6})\kappa_{T,nC12} \quad (17)$$

Where $\emptyset_{nC6}$ is the volume fraction of n-hexane in the binary mixture defined by:

$$\emptyset_{nC6} = \frac{x_{nC6}M_{nC6}}{\rho_{nC6}\sum_i x_i \frac{M_i}{\rho_i}} \quad (18)$$

Where the subscript *i* denotes either n-hexane or n-dodecane.

It has been obtained that experimental κ_T^E values are negative in our pressure and temperature range. This is consistent with the negative values of excess molar volumes which implies that the real mixtures are denser so less compressible than the ideal mixtures. Interestingly, although

κ_T^E values are often very small, they can become sometimes significant relatively to the real mixture values of κ_T, reaching up to 25% at T = 313.15 K and P = 0.1 MPa, see Fig. 6. Furthermore, we evaluated the capability of molecular simulations to describe the non-ideal behaviour of the mixture in terms of κ_T. The results are in good adequacy with experimental one, as depicted by Fig.6 where comparison are performed for the highest values of relative excess isothermal compressibility (κ_T^E/κ_T). In this figure, both force fields, depict the same trend as the experimental values, except at 80 % of n-hexane for which the molecular simulations underestimate noticeably the experimental value. These observations are further evidence of the consistency of the simple Lorentz-Berthelot rule to describe the studied mixture.

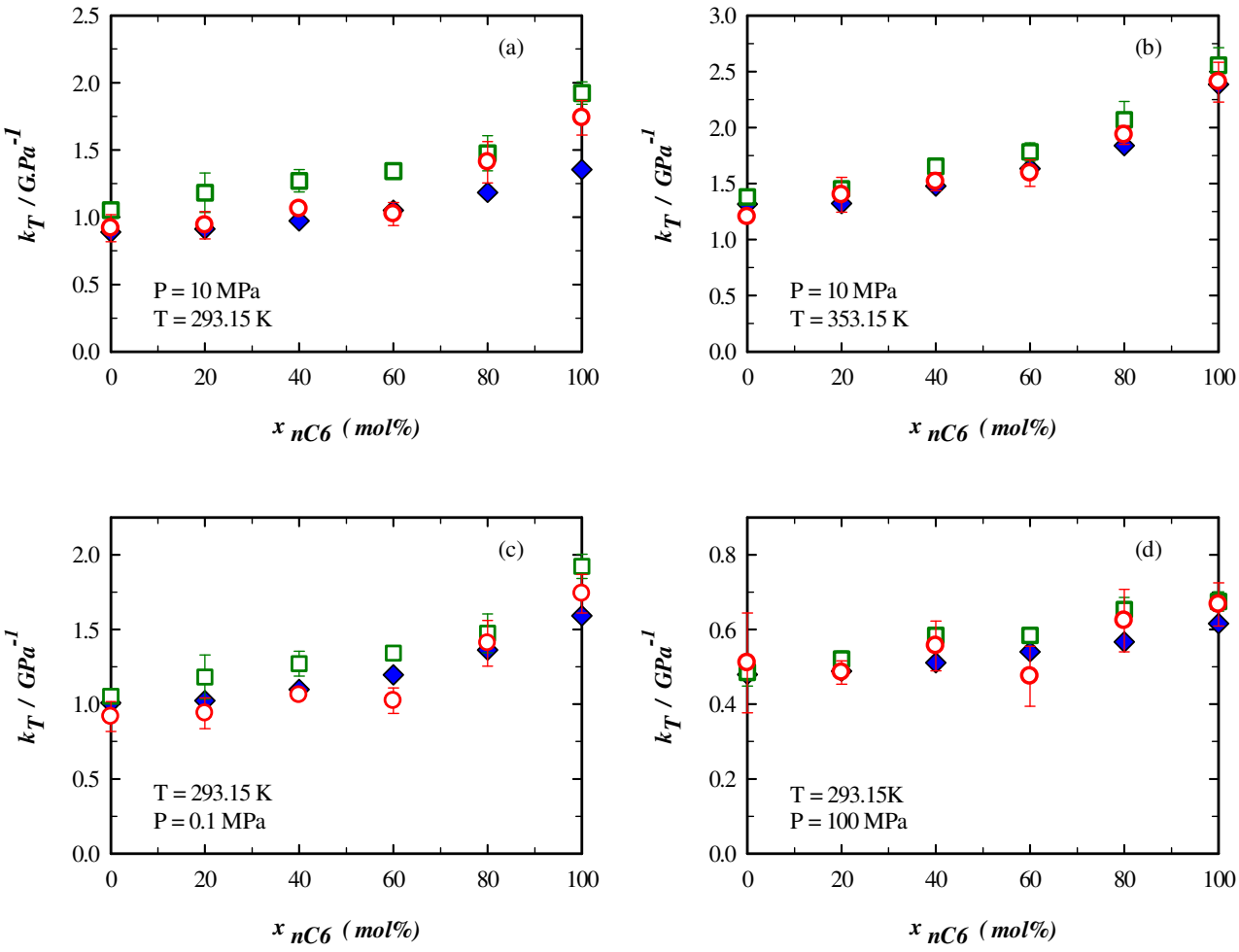

Fig. 5 Isothermal compressibility as a function of n-hexane concentration at different temperature and pressure conditions. Comparison between ◆: experimental data; □: TraPPE-ua and ○: MCCG.

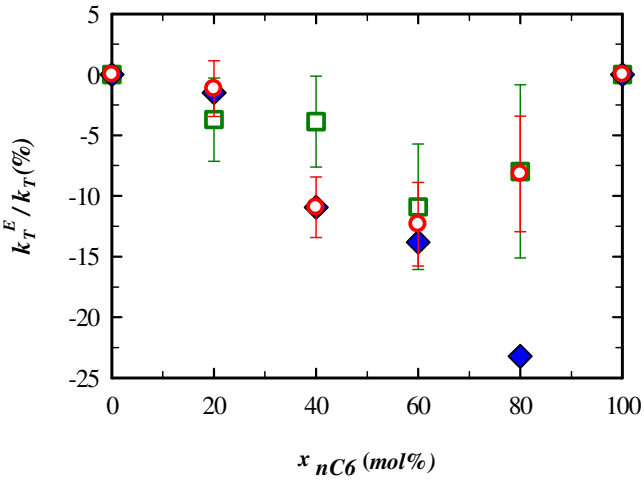

Fig. 6 Relative excess isothermal compressibility as a function of concentration of n-hexane at 333.15 K and 0.1MPa. Comparison between data calculated from ◆: experimental data; □: TraPPE-ua and ○: MCCG .

3.1.3. Speed of sound

In this section, simulation results reported in Tables S.11 and S.12 were compared to experimental speed of sound. Numerical speed of sound was computed indirectly according to Newton-Laplace equation (Eq. (11)) using density, isothermal compressibility, isobaric thermal expansion and residual heat capacity directly estimated from Monte Carlo simulations. The use of this method, notwithstanding that it leads to important expanded uncertainties, provides generally acceptable results even if appears as indirect[52]. The parity plot of Fig.7 shows that the MCCG force field is more efficient to predict the speed of sound than the TraPPE-ua. The latter, as depicted more clearly by Fig. 8, systematically underestimates this property with a Bias of 6.1 % and an AAD of 6.1 % while for MCCG the Bias is of 0.1 % and the AAD is equal to 2.5 %.

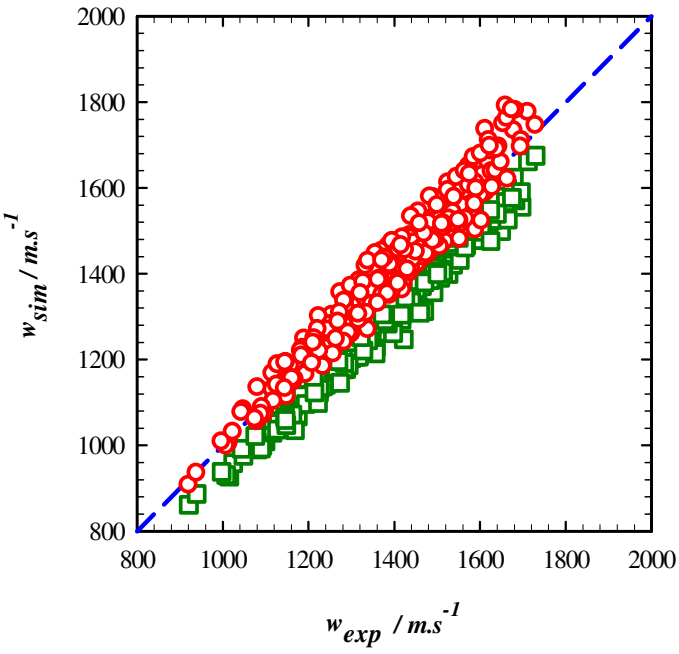

Fig. 7 Molecular simulation data of speed of sound w_{sim} as a function of experimental data w_{exp} for the mixture n-hexane + n-dodecane. Comparison between □: TraPPE-ua and ○: MCCG .

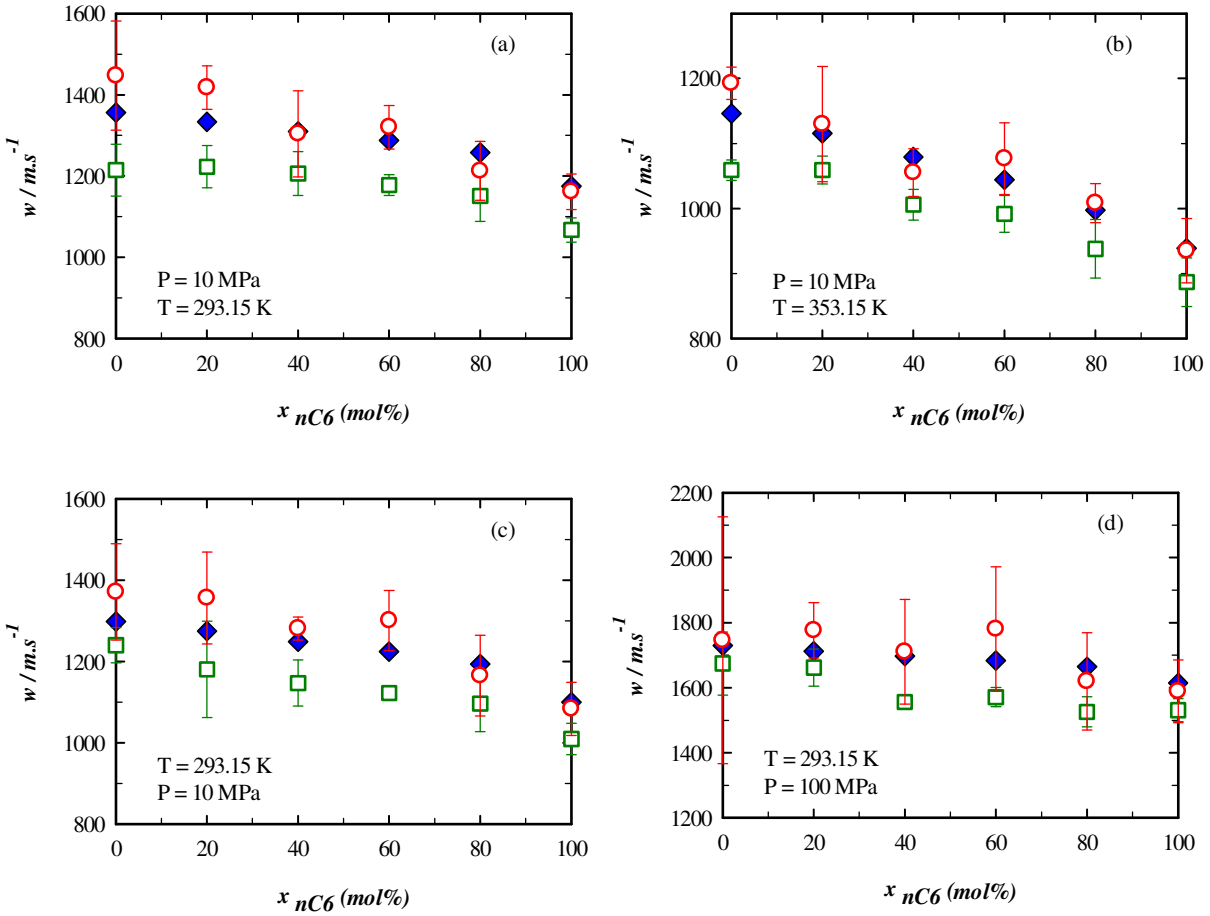

Fig. 8 Speed of sound as a function of n-hexane concentration at different temperature and pressure conditions. Comparison between ◆: experimental data; □: TraPPE-ua and ○: MCCG.

Thereafter, we calculated the excess speed of sound w^E in the mixture . However, contrary to excess molar volume and isothermal compressibility, the calculation of w^E is not straightforward. The corresponding equation, which is presented in more details in a previous paper[53] is defined as follows:

$$w^E = w - \sqrt{\frac{\sum_i x_i \frac{M_i}{\rho_i}}{M\kappa_S^{id}}} \tag{19}$$

With

$$\kappa_S^{id} = \sum_i \emptyset_i \kappa_{T,i} - \frac{\left(\sum_i x_i \frac{M_i}{\rho_i}\right)\left(\sum_i \emptyset_i \alpha_{p,i}\right)^2}{\sum_i x_i \frac{M_i T \alpha_{p,i}^2}{\rho_i\left(\kappa_{T,i} - \kappa_{S,i}\right)}} \tag{20}$$

In addition to density ρ_i and isothermal compressibility $\kappa_{T,i}$, Eq. (20) also involves the isentropic compressibility $\kappa_{S,i}$ and the isobaric thermal expansion $\alpha_{p,i}$. The first one is calculated from the speed of sound and the density according to the following relation:

$$\kappa_{S,i} = \frac{1}{\rho_i w_i^2} \tag{21}$$

Concerning the isobaric thermal expansion, it was obtained from derivation of isobaric density measurements with respect to temperature by using the same Monte Carlo derivation method as the isothermal compressibility.

As indicated in Fig.9 for the most pronounced case (T = 313.15 K and P = 0.1 MPa), the experimental excess speed of sound values are positive. This behavior perfectly matches with our observations on excess molar volume and excess isothermal compressibility. Indeed, v^E and κ_T^E were shown to be negative, which means that the real mixture is denser than the ideal one, leading to higher speed of sound in the former. In terms of amplitude, the excess sound velocity data can reach up to 6% of real mixture values as depicted in Fig. 6. Then, numerical

excess speed of sound values were calculated from simulation results for both force fields by applying Eqs. (18) and (19). Such calculation exhibits very large error bars (up to 150 m/s) that are probably overestimated due to the fact that simulations results are correlated**.** In Fig.9, simulation relative excess sound velocities are compared to experimental ones. Interestingly, the simulations values follow the trends depicted by the experimental results and are of the same order of magnitude, showing the ability of the simulations to capture the weak non-ideal behavior of the mixture in terms of such an indirect property.

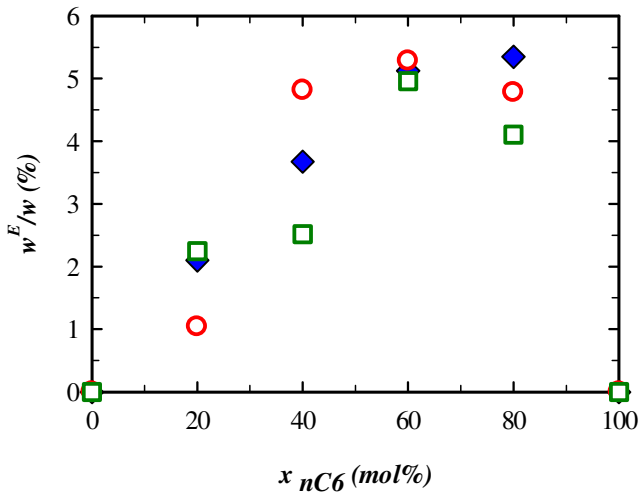

Fig. 9 Relative excess sound velocity as a function of concentration of n-hexane at 333.15 K and 0.1MPa. Comparison between data calculated from ◆: experimental data; □: TraPPE-ua and ○: MCCG. For the sake of clarity, the large error bars are not represented.

3.2. Shear Viscosity

As a further test of the capabilities of the chosen force fields, we evaluated their performance using Molecular Dynamic simulations combined to experimental measurements, to predict the viscosity of n-hexane and n-dodecane and their binary mixtures. The simulations were performed at two temperatures (293.15 and 353.15 K) and five pressures (0.1, 10, 40, 70 and 100 MPa). The results with their corresponding numerical standard deviations for both TraPPE-

ua and MCCG force fields are summarized in Tables S.13 and S.14 of SI. Comparisons to experimental data in Figs.10 and 11 reveal that simulations with both force fields systematically underpredict the viscosity, with underestimations reaching 50 %. More precisely, for both molecular models, the denser (low temperature, high pressure, high content of n-dodecane) the system is, the higher are the deviations from experimental data as depicted by Fig. 11.

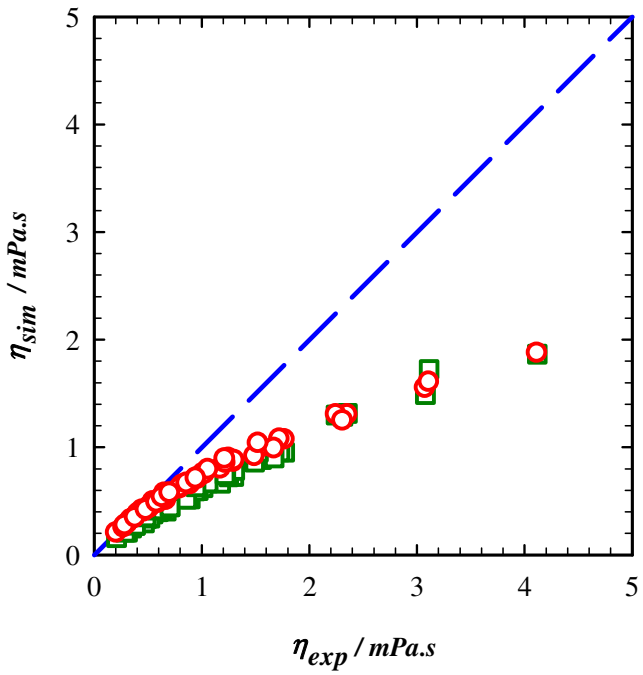

Fig. 10 Molecular simulation data of viscosity η_{sim} as a function of experimental data η_{exp} for the mixture n-hexane + n-dodecane. Comparison between □: TraPPE-ua and ○: MCCG.

The MCCG force field appears to be slightly more accurate than TraPPE-ua for low viscosities, see Fig. 11. Quantitatively the experimental viscosities are underestimated by MCCG with an overall AAD of 24 %, a Bias of 24 % and a Max AD of 50 % whereas for TraPPE-ua an overall AAD of 35 %, a Bias of 35 % and a Max AD of 55 % are observed. Such a weakness of some force fields to yield correct transport properties has already been noticed by many authors[10,13,14,54–57] for n-alkanes systems. This inability of both force fields to capture correctly

the density dependence of shear viscosity of such systems is related to the way the force fields describe the molecules' global rigidity[10,13]. Indeed, most of the force fields, including TraPPE-ua, have been developed so as to mimic essentially equilibrium properties. However, it is known that phase equilibrium properties are usually less dependent to the internal rigidity than is viscosity[10] and so are not discriminative properties regarding the way internal degrees of freedom should be described.

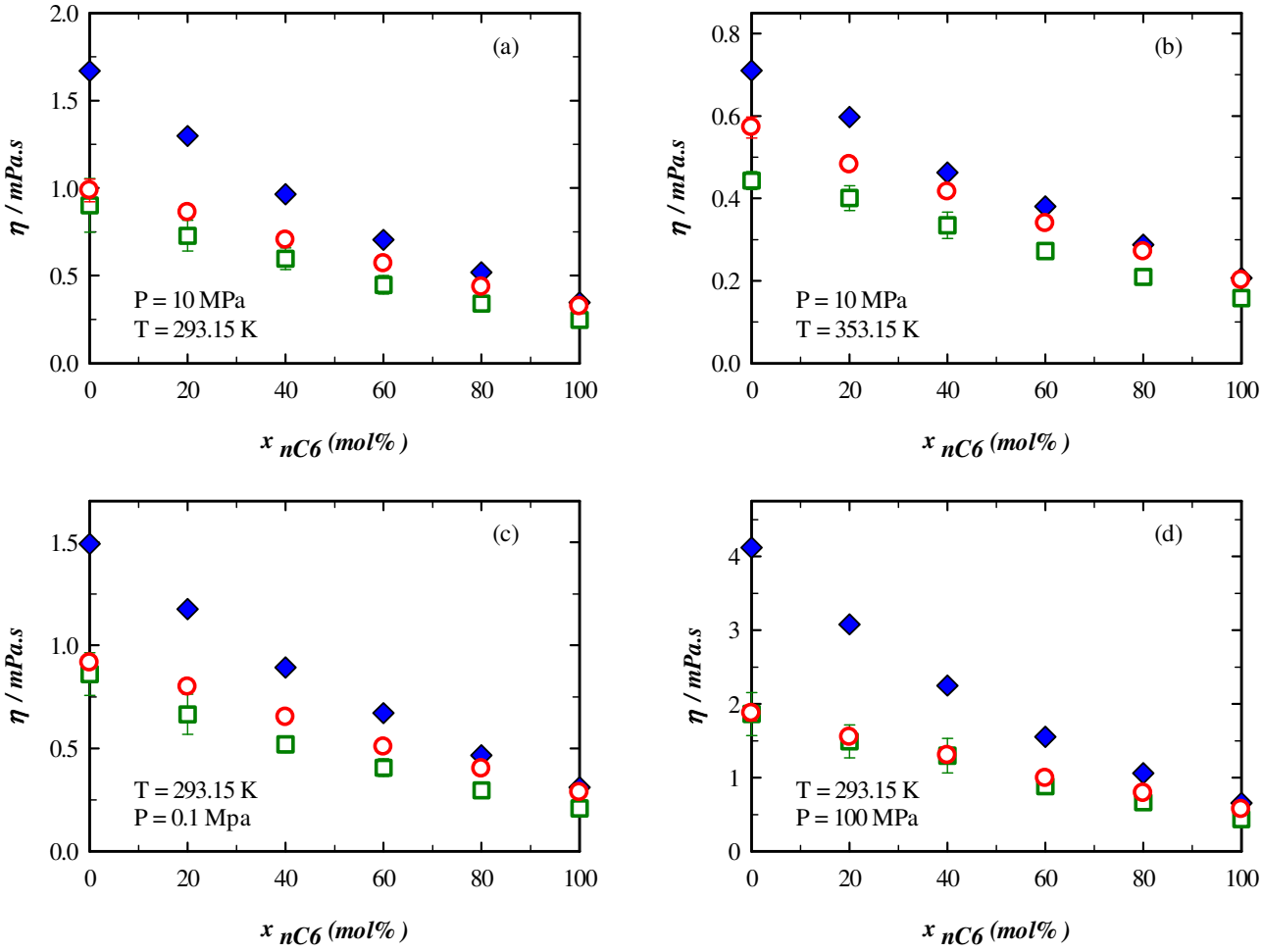

Fig. 11 Viscosity as a function of n-hexane concentration at different temperature and pressure conditions. Comparison between ◆: experimental data; □: TraPPE-ua and ○: MCCG .

As for thermodynamic properties, we defined a viscosity deviation called excess viscosity of the binary mixture as the difference between the real mixture viscosity and a linear combination of pure compound viscosities[58], i.e. :

$$\eta^E = \eta - x_{nC6}\eta_{nC6} - (1 - x_{nC6})\eta_{nC12} \quad (22)$$

It should be noticed that such an "excess" viscosity definition is not unique and has been chosen simply by analogy to the excess properties used to describe deviation from ideal mixtures on the volumetric properties as both quantities are strongly linked.

As expected, the experimental results show that the excess viscosities are negative. This is because the dispersion forces are dominant in the studied mixture [59,60]**.** The excess viscosities decrease in absolute values as the pressure is decreased and the temperature is increased. Consequently , the maximum absolute values of η^E in our range of temperature and pressure are observed at 293.15 K and 100 MPa, corresponding to the smallest values of v^E, κ_T^E and w^E. In these conditions, the excess viscosity can reach up to 35% of the real mixture viscosity. Fig.12 compares the simulation relative excess viscosities to experimental values in the case of highest values of η^E . It appears that the excess viscosity is not well quantified by the MCCG force field and is only qualitatively captured (noticeably underestimated in absolute value) by the TraPPE-ua. This misevaluation, even if small compared to the ones noticed on pure fluids, adds to the limitations of these force fields to predict accurately viscosity for the densest systems studied here and may indicate a limitation of the combining rules used in this work. Such results highlight that viscosity is an interesting and sensitive property not only to evaluate the quality of force field but also the capabilities of combining rules to capture cross interactions for a given molecular model.

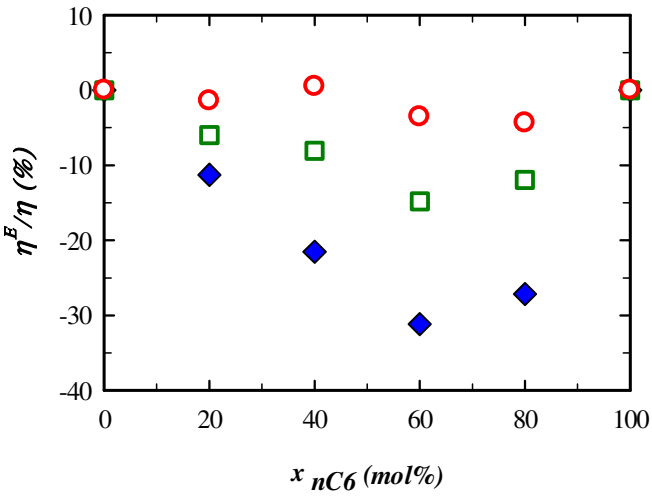

Fig. 12 Relative excess viscosity as a function of concentration of n-hexane at 293.15 K and 100 MPa. Comparison between data calculated from ◆: experimental data; □: TraPPE-ua and ○: MCCG . For the sake of clarity, the large error bars are not represented.

4. CONCLUSIONS

In this work, we have evaluated the capabilities of two force fields, a united atom one (TraPPE-ua) and a coarse grained one (MCCG), to provide simultaneously thermodynamic properties, including derivative ones and excess quantities, and shear viscosity of simple liquid mixtures composed of n-hexane + n-dodecane over a wide range of thermodynamic conditions (from 293.15 to 353.15 K and pressure up to 100 MPa). To achieve this test on a consistent and controlled set of data, we have performed accurate measurements of density, speed of sound and shear viscosity of these mixtures. From the simulation point of view, we have computed the aforementioned thermophysical properties at the same thermodynamic conditions using both classical Monte Carlo and Molecular Dynamics simulations combined with the two tested force fields and simple Lorentz-Berthelot combining rules.

The results obtained by the TraPPE-ua force field yield an AAD of 1.5% for the density, 11.1% for the isothermal compressibility, 6.1% for the sound velocity and 35% for the viscosity. Concerning the MCCG force field, it leads to slightly better results with an AAD of, 1.2% for the density, 5.9% for the isothermal compressibility, 2.5% for the speed of sound and 24% for the viscosity. An additional interesting point is that, when comparing the simulated excess properties to experimental values, the two force fields, using simple Lorentz Berthelot combining rules, are shown to capture rather well the weak non-ideality of the mixtures in terms of excess thermodynamic properties, but not in terms of excess viscosity. Thus, these results validate that both TraPPE-ua and MCCG are able to yield results on direct and derivative thermodynamic properties in fair agreement with experimental ones. However, important deviations (systematic underestimation) from experimental data, up to around 50 %, are observed on viscosity for the densest systems. Such deviations confirm that, even on simple molecular systems such as n-alkane mixtures, force fields that are able to describe accurately fluid equilibrium properties are not always able to yield precise transport properties. Consequently, viscosity is an interesting property not only to evaluate the quality of force fields but also to assess the capabilities/limitations of the combining rules to capture cross interactions for a given molecular model.

Further systematic tests are planned to deal with more asymmetric, and so more non-ideal mixtures[53,61], which are known to be even more difficult to model using classical equation of states and viscosity correlations, approaches [2]. This will be achieved in the future together with a more systematic test of various possibilities for the combining rules for the MCCG force field as this should impact the results when dealing with asymmetric mixtures. Finally, to improve the prediction capability for the viscosity, the MCCG force field will be further extended by introducing a rigidity parameter as already initiated in ref [10].

ACKNOWLEDGEMENTS

We gratefully acknowledge the "Communauté d'Agglomération de Pau-Pyrénées" for the PhD grant allowed to one of the authors, Abdoul Wahidou Saley Hamani and Scienomics for the free availability of the MAPS software.

APPENDIX A: SUPPLEMENTARY MATERIALS

Supplementary information related to this article can be found in a separated file.

REFERENCES

(1) M. Lagache, P. Ungerer, A. Boutin and A. H. Fuchs, Prediction of Thermodynamic Derivative Properties of Fluids by Monte Carlo Simulation, Phys. Chem. Chem. Phys. **3** (2001) 4333.

(2) E. Hendriks, G. M. Kontogeorgis, R. Dohrn, J. C. de Hemptinne, I. G. Economou, L. F. Žilnik, V. Vesovic, Industrial Requirements for Thermodynamics and Transport Properties, Ind. Eng. Chem. Res. **49** (2010) 11131.

(3) Ø. Wilhelmsen, A. Aasen, G. Skaugen, P. Aursand, A. Austegard, E. Aursand, M. A. Gjennestad, H. Lund, and M. Hammer, Thermodynamic Modeling with Equations of State: Present Challenges with Established Methods, Ind. Eng. Chem. Res. **56** (2017) 3503.

(4) T. Yang, Ø. Fevang, K. Christoffersen, E. Ivarrud, LBC Viscosity Modeling of Gas Condensate to Heavy Oil, SPE-109892-MS (2007).

(5) M. Assael, A. R. H. Goodwin, V. Vesovic, W. A. Wakeham, Experimental Thermodynamics Volume IX: Advances in Transport Properties of Fluids, 1st Ed., Royal Society of Chemistry, Cambridge, 2014.

(6) K. E. Gubbins and J. D. Moore, Molecular Modeling of Matter: Impact and Prospects in Engineering, Ind. Eng. Chem. Res. **49** (2010) 3026.

(7) P. Ungerer, C. Nieto-Draghi, B. Rousseau, G. Ahunbay, V. Lachet, Molecular Simulation of the Thermophysical Properties of Fluids: From Understanding Toward Quantitative Predictions. J. Mol. Liq. **134** (2007) 71.

(8) M. G. Martin, J. I. Siepmann, Transferable Potentials for Phase Equilibria. 1. United-Atom Description of n-Alkanes, J. Phys. Chem. B **102** (1998) 2569.

(9) H. Hoang, S. Delage-Santacreu, G. Galliero, Simultaneous Description of Equilibrium, Interfacial, and Transport Properties of Fluids Using a Mie Chain Coarse-Grained Force Field, Ind. Eng. Chem. Res. **56** (2017) 9213.

(10) G. Galliero, Equilibrium, Interfacial and Transport Properties of n-Alkanes: Towards the Simplest Coarse Grained Molecular Model, Chem. Eng. Res. Des. **92** (2014) 3031.

(11) A. Mejía, C. Herdes, E. A. Müller, Force Fields for Coarse-Grained Molecular Simulations from a Corresponding States Correlation, Ind. Eng. Chem. Res. **53** (2014) 4131.

(12) T. Lafitte, A. Apostolakou, C. Avendaño, A. Galindo, C. S. Adjiman, E. A. Müller, G. Jackson, Accurate Statistical Associating Fluid Theory for Chain Molecules Formed from Mie Segments, J. Chem. Phys. **139** (2013) 154504.

(13) C. Nieto-Draghi, P. Ungerer, B. Rousseau, Optimization of the Anisotropic United Atoms Intermolecular Potential for N-Alkanes: Improvement of Transport Properties, J. Chem. Phys. **125** (2006) 044517.

(14) R. A. Messerly, M. C. Anderson, S. M. Razavi, J. R. Elliott, Improvements and Limitations of Mie λ-6 Potential for Prediction of Saturated and Compressed Liquid Viscosity, Fluid Phase Equilib. **483** (2019) 101.

(15) B. Lagourette, C. Boned, H. Saint-Guirons, P. Xans, H. Zhou, Densimeter Calibration Method versus Temperature and Pressure, Meas. Sci. Technol. **3** (1992) 699.

(16) C.E. Kuyatt, B.N. Taylor, Guidelines for Evaluating and Expressing the Uncertainty of NIST Measurement Results, NIST Tech. Note (1994) 1297.

(17) J.-L. Daridon, J.-P. Bazile, Computation of Liquid Isothermal Compressibility from Density Measurements: An Application to Toluene, J. Chem. Eng. Data **63** (2018) 2162.

(18) J.-P. Bazile, D. Nasri, J.-L. Daridon, Speed of Sound, Density, and Derivative Properties of Tris(2-Ethylhexyl) Trimellitate under High Pressure, J. Chem. Eng. Data **62** (2017) 1708.

(19) P. Daugé, A. Baylaucq, L. Marlin, C. Boned, Development of an Isobaric Transfer Viscometer Operating up to 140 MPa. Application to a Methane + Decane System, J. Chem. Eng. Data **46** (2001) 823.

(20) M. P. Allen, D. J. Tildesley, Computer Simulation of Liquids, 2nd Ed. Oxford University Press, Oxford, 2017.

(21) D. Frenkel, B. Smit, Understanding Molecular Simulation, 2nd Ed., Acad. Press, Cambridge, 2002.

(22) G. Galliero, C. Boned, A. Baylaucq, F. Montel, Molecular dynamics comparative study of Lennard-Jones alpha-6 and exponential alpha-6 potentials: Application to real simple fluids (viscosity and pressure), Phys. Rev. E **73** (2006), 061201.

(23) G. Galliero, C. Boned, Molecular dynamics study of the repulsive form influence of the interaction potential on structural, thermodynamic, interfacial and transport properties, J. Chem. Phys. **129** (2008), 074506.

(24) J. E. Lennard-Jones, On the Determination of Molecular Fields, Proc. R. Soc. Lond. **106** (1924) 441.

(25) J. E. Lennard-Jones, Cohesion, Proc. Phys. Soc. **43** (1931) 461.

(26) H. A. Lorentz, Ueber die Anwendung des Satzes vom Virial in der kinetischen Theorie der Gase, Ann. Phys. **1** (1881) 248.

(27) D. Berthelot, Sur le mélange des gaz, Comptes rendus hebdomadaires des séances de l'Académie des Sciences **126** (1898) 1703.

(28) C. J. Mundy, S. Balasubramanian, K. Bagchi, J. I. Siepmann, M. L. Klein, Equilibrium and Non-Equilibrium Simulation Studies of Fluid Alkanes in Bulk and at Interfaces, Faraday Discuss. **104** (1996) 17.

(29) M. S. Kelkar, J. L. Rafferty, E. J. Maginn, J. Ilja Siepmann, Prediction of Viscosities and Vapor–Liquid Equilibria for Five Polyhydric Alcohols by Molecular Simulation, Fluid Phase Equilib. **260** (2007) 218.

(30) G. Mie, Zur kinetischen Theorie der einatomigen Köper Ann. Phys. 316 (1903) 657.

(31) G. Galliero, H. Bataller, J.-P. Bazile, J. Diaz, F. Croccolo, H. Hoang, R. Vermorel, P.-A. Artola, B. Rousseau, V. Vesovic, et al. Thermodiffusion in Multicomponent n -Alkane Mixtures. Npj Microgravity **3** (2017) 1.

(32) G. Galliero, T. Lafitte, D. Bessieres, C. Boned, Thermodynamic properties of the Mie n-6 fluid : A comparison between statistical associating fluid theory of variable range approach and molecular dynamics results, J. Chem. Phys. **127** (2007) 184506.

(33) S. Delage-Santacreu, G. Galliero, H. Hoang, J.P. Bazile, C. Boned, J. Fernandez. Thermodynamic scaling of the shear viscosity of Mie n-6 fluids and their binary mixtures, J. Chem. Phys. **142** (2015) 174501.

(34) H. Hoang, P. Nguyen, M. Pujol, G. Galliero, Elemental and isotopic fractionation of noble gases in gas and oil under reservoir conditions: Impact of thermodiffusion, Eur. Phys. J. E. **42** (2019) 61.

(35) P. Ungerer, B. Tavitian; A. Boutin, Applications of molecular simulations in the oil and gas industry, Monte Carlo methods. Ed. TECHNIP, Paris, 2005.

(36) T. J. H. Vlugt; M.G. Martin, B. Smit; and R. Krishna, J. I. Siepmann, Improving the Efficiency of the Configurational-Bias Monte Carlo Algorithm, Mol. Phys. **94** (1998) 727.

(37) J. I. Siepmann, D. Frenkel, Configurational Bias Monte Carlo: A New Sampling Scheme for Flexible Chains, Mol. Phys. **75** (1992) 59.

(38) C. D. Wick, J. I. Siepmann, Self-Adapting Fixed-End-Point Configurational-Bias Monte Carlo Method for the Regrowth of Interior Segments of Chain Molecules with Strong Intramolecular Interactions, Macromolecules **33** (2000) 7207.

(39) Y. Mishin, Thermodynamic Theory of Equilibrium Fluctuations, Ann. Phys. **363** (2005) 48.

(40) J. S. Rowlinson, F. L. Swinton, J. E. Baldwin, A. D. Buckingham, S. Danishefsky, Liquids and Liquid Mixtures: Butterworths Monographs in Chemistry, 3rd ed., Butterworth-Heinemann Ltd: London, Boston, 1982.

(41) E.W. Lemmon, I.H. Bell, M.L. Huber, M.O. McLinden, NIST Standard Reference Database 23: Reference Fluid Thermodynamic and Transport Properties-REFPROP, Version 8.0, National Institute of Standards and Technology, Standard Reference Data Program, Gaithersburg, 2007.

(42) M. G. Martin, MCCCS Towhee: A Tool for Monte Carlo Molecular, 2013. See http://towhee.sourceforge.net

(43) F. Müller-Plathe, Reversing the Perturbation in Nonequilibrium Molecular Dynamics: An Easy Way to Calculate the Shear Viscosity of Fluids, Phys. Rev. E **59** (1999) 4894.

(44) S. Nosé, A Unified Formulation of the Constant Temperature Molecular Dynamics Methods, J. Chem. Phys. **81** (1984) 511.

(45) D. J. Evans, B. L. Holian, The Nose–Hoover Thermostat, J. Chem. Phys. **83** (1985) 4069.

(46) W. G. Hoover, Canonical Dynamics: Equilibrium Phase-Space Distributions, Phys. Rev. A **31** (1985) 1695.

(47) H. J. C. Berendsen, J. P. M. Postma, W. F. van Gunsteren, A. Di Nola, J. R. Haak, Molecular Dynamics with Coupling to an External Bath, J. Chem. Phys. **81** (1984) 3684.

(48) H. C. Andersen, Rattle: A "Velocity" Version of the Shake Algorithm for Molecular Dynamics Calculations, J. Comput. Phys. **52** (1983) 24.

(49) S. Plimpton, Fast Parallel Algorithms for Short-Range Molecular Dynamics, J. Comput. Phys. **117** (1995) 1.

(50) A. J. Treszczanowicz, O. Kiyohara, G. C. Benson, Excess Volumes for N-Alkanols +n-Alkanes IV. Binary Mixtures of Decan-1-Ol +n-Pentane, +n-Hexane, +n-Octane, +n-Decane, and +n-Hexadecane, J. Chem. Thermodyn. **13** (1981) 253.

(51) M. Nakamura, K. Chubachi, K. Tamura, S. Murakami, Excess Molar Volumes, Excess Isentropic and Isothermal Compressibilities, and Excess Molar Isochoric Heat Capacities of [XCF3CH2OH + (1-x) {HCON(CH3)2 or CH3CN}] at the Temperature 298.15 K, J. Chem. Thermodyn. **25** (1993) 525.

(52) B. Fazelabdolabadi, A. Bahramian, Prediction of Sound Velocity in Normal Alkanes: A Configurational-Bias Monte Carlo Simulation Approach, Fluid Phase Equilib. **284** (2009) 129.

(53) J.-P. Bazile, D. Nasri, A. W. Saley Hamani, G. Galliero, J.-L. Daridon, Excess Volume, Isothermal Compressibility, Isentropic Compressibility and Speed of Sound of Carbon Dioxide + n-Heptane Binary Mixture under Pressure up to 70 MPa. I Experimental Measurements, J. Supercrit. Fluids **140** (2018) 218.

(54) G. Galliero, (2014), Computer Simulations, in: M. J. Assael, A. R. H. Goodwin, V. Vesovic, W. A. Wakeham (Eds.), Experimental Thermodynamics Volume IX: Advances in Transport Properties of Fluids, 1st ed., R. Soc. of Chem., Cambridge, 362–386.

(55) W. Allen, R. L. Rowley, Predicting the Viscosity of Alkanes Using Nonequilibrium Molecular Dynamics: Evaluation of Intermolecular Potential Models, J. Chem. Phys. **106** (1997) 10273.

(56) D. K. Dysthe, A. H. Fuchs, B. Rousseau, M. Durandeau, Fluid Transport Properties by Equilibrium Molecular Dynamics. II. Multicomponent Systems, J. Chem. Phys. **110** (1999) 4060.

(57) S. Rahman, O. Lobanova, G. Jiménez-Serratos, C. Braga, V. Raptis, E. A. Müller, G. Jackson, C. Avendaño, A. Galindo, SAFT-γ Force Field for the Simulation of Molecular Fluids. 5. Hetero-Group Coarse-Grained Models of Linear Alkanes and the Importance of Intramolecular Interactions, J. Phys. Chem. B **122** (2008) 9161.

(58) B. Garcia, J. C. Ortega, Excess Viscosity η^E, Excess Volume V^E, and Excess Free Energy of Activation ΔG^E at 283, 293, 303, 313, and 323 K for Mixtures Acetonitrile and Alkyl Benzoates, J. Chem. Eng. Data **33** (1988) 200.

(59) S. Verma, S. Gahlyan, M. Rani, S. Maken, Transport Properties and Modeling of Viscosity for Binary Mixtures of Butanol Isomers + Hydrocarbons, Arab. J. Sci. Eng. **43** (2018) 6087.

(60) R. J. Fort, W. R. Moore, Viscosities of Binary Liquid Mixtures, Trans. Faraday Soc. **62** (1966) 1112.

(61) T. Regueira, G. Pantelide, W. Yan, E. H. Stenby, Density and Phase Equilibrium of the Binary System Methane + N-Decane under High Temperatures and Pressures, Fluid Phase Equilib. **428** (2016) 48.